Chem Biol Drug Des 2016; **87:** 694–703

Research Article

Discovery of 1,3-Diaryl-pyridones as Potent VEGFR-2 Inhibitors: Design, Synthesis, and Biological Evaluation

Wei Yan[1,†], Zhaoru Huang[2,3,†], Zhengyu Wang[4], Sufen Cao[1], Linjiang Tong[2], Tao Zhang[2], Chen Wang[5], Lin Zhou[3], Jian Ding[2], Cheng Luo[5,*], Jinpei Zhou[4,*], Hua Xie[2,*] and Wenhu Duan[1,6,*]

[1]School of Pharmacy, East China University of Science & Technology, Shanghai 200237, China
[2]Division of Anti-Tumor Pharmacology, State Key Laboratory of Drug Research, Shanghai Institute of Materia Medica, Shanghai 201203, China
[3]Department of Gastroenterology, The First Affiliated Hospital of Zhengzhou University, Zhengzhou, Henan Province 450014, China
[4]Department of Medicinal Chemistry, China Pharmaceutical University, Nanjing 210009, China
[5]Drug Discovery and Design Center, State Key Laboratory of Drug Research, Shanghai Institute of Materia Medica, Shanghai 201203, China
[6]Department of Medicinal Chemistry, Shanghai Institute of Materia Medica, Shanghai 201203, China
**Corresponding authors: Cheng Luo, cluo@simm.ac.cn; Jinpei Zhou, jpzhou668@163.com; Hua Xie, hxie@simm.ac.cn; Wenhu Duan, whduan@simm.ac.cn*
[†]These authors contributed equally to this work.

In this study, we described the design, synthesis, and biological evaluation of 1,3-diaryl-pyridones as vascular endothelial growth factor receptor-2 (VEGFR-2) inhibitors. The 1,3-diaryl-pyridones were synthesized via Chan-Lam and Suzuki coupling reactions. Two representative compounds, 17 and 35h, displayed excellent enzymatic inhibitory activities, with IC_{50} values of 3.5 and 3.0 nM, respectively. Furthermore, compounds 17 and 35h blocked the tube formation and suppressed the VEGF-induced phosphorylation of VEGFR-2 and downstream extracellular signal-regulated kinases (Erk) in human umbilical vein endothelial cells (HUVECs) at 10 nM concentration. The docking simulation showed that compound 17 bound well into the active site of VEGFR-2 via two hydrogen bonds and hydrophobic interactions.

Key words: 1,3-Diaryl-pyridone, angiogenesis, anticancer agent, Chan-Lam coupling, VEGFR-2 inhibitors

Received 15 July 2015, revised 4 November 2015 and accepted for publication 3 December 2015

Angiogenesis, the process of forming new blood vessels from existing ones, is a normal physiological process that occurs during embryogenesis, wound healing, and the menstrual cycle (1). Aberrant angiogenesis, however, plays a critical role in tumor cell proliferation, invasion, and metastasis (2–4). New blood capillaries are required by solid tumors to supply nutrient, remove metabolic waste, and facilitate metastasis formation (2,3,5). Therefore, the inhibition of tumor angiogenesis has been proven to be a reliable approach for the treatment of cancers (6,7).

Vascular endothelial growth factor (VEGF) and its receptor (VEGFR) are settled to be key intermediates of angiogenesis. Overexpression of VEGF correlates with poor prognosis and clinical stage in patients with solid tumors (8–10). Binding of VEGF to VEGFR-2 triggers a cascade of downstream signaling pathway that finally leads to angiogenesis, tumor proliferation, and migration (11,12). Inhibition of angiogenesis by the blockage of VEGF/VEGFR-2 signaling pathway has been utilized as a valuable approach in the treatment of cancers. In the past decade, several small molecule VEGFR-2 inhibitors have been approved, for example, sunitinib (13), sorafenib (14), and pazopanib (15), or have entered late stage clinical trials, for example, tivozanib (16) and linifanib (17).

Recent studies of VEGFR-2 inhibitors have been focused on exploring different scaffolds that bind to the hinge region, and several new scaffolds have been utilized to generate potent VEGFR-2 inhibitors, for example, quinoxalines (18), pyrazolo[3,4-*d*]pyrimidines (19,20), pyrazolylamines (21), nicotinamides (22), and thiazolo[5,4-*d*]pyrimidines (23). However, modifications on the linker between hinge region and the hydrophobic pocket were rarely reported. The urea moiety was mainly kept unchanged because it could form three hydrogen bonds with Clu-885 and Asp-1046 (24). Therefore, the urea moiety seemed to be a 'restricted area' for modification.

Researchers from Amgen Inc. (Thousand Oaks, CA, USA) have developed two series of potent VEGFR-2 inhibitors (25,26). In both series, one of the NHs in the urea moiety is cyclized with the middle phenyl ring either to form naphthamides or to form 2,3-dihydro-4*H*-benzo[*b*][1,4]oxazine-4-carboxamides while maintaining the potency (IC_{50} values

 doi: 10.1111/cbdd.12703

of 0.5 nM for compounds **1** and **2**) (Figure 1, cyclization pattern 1). This phenomenon was also found to be consistent with our previous study (27). In view of these facts, we envisioned that cyclization of the urea moiety to form pyridones (Figure 1, cyclization pattern 2) would also be acceptable. Herein, we described the discovery of 1,3-diaryl-pyridone derivatives as potent VEGFR-2 inhibitors.

Methods and Materials

Chemistry

All reagents and solvents were purchased from commercial suppliers and used without further purification unless otherwise noted. Flash chromatography was performed using silica gel (300–400 mesh). ^{1}H NMR spectral data were recorded on Varian Mercury 300 or 400 MHz NMR spectrometer, and ^{13}C NMR spectral data were recorded on Varian Mercury 101 or 126 MHz NMR spectrometer. Chemical shifts (δ) were reported in parts per million using TMS as the internal standard. The high-resolution mass spectra were recorded on a Finnigan/MAT95 spectrometer.

General procedure for the synthesis of compounds 7a–g

To a mixture of 3-bromopyridin-2(1*H*)-one (**5**) (174 mg, 1 mmol), (4-fluorophenyl)boronic acid (210 mg, 1.5 mmol), and pyridine (158 mg, 2 mmol) in CH_2Cl_2 (10 mL) was added $Cu(OAc)_2$ (40 mg, 0.2 mmol) and 4 Å molecular sieves (50 mg). The resulting mixture was stirred in the open air overnight. The reaction mixture was filtered, and the filtrate was concentrated under reduced pressure. The resulting residue was purified by silica gel chromatography (CH_2Cl_2/MeOH 99:1 v:v) to give **7a** (206 mg, 77%) as a white solid (28). ^{1}H NMR (300 MHz, $CDCl_3$) δ 7.81 (dd, J = 7.2, 1.9 Hz, 1H), 7.40–7.30 (m, 3H), 7.17 (t, J = 8.5 Hz, 2H), 6.16 (t, J = 7.0 Hz, 1H).

Compounds **7b–g** were prepared following the same procedure as described for the synthesis of compound **7a**, and the analytical data were summarized in supporting information.

Synthesis of 1-benzyl-3-bromopyridin-2(1*H*)-one (7h)

Sodium hydride (60% in mineral oil, 172 mg, 4.3 mmol) was suspended in DMF (10 mL), and 3-bromopyridin-2(1*H*)-one (**5**) (500 mg, 2.9 mmol) was added portionwise at 0 °C. Benzyl bromide (983 mg, 5.7 mmol) was added, and the mixture was stirred at ambient temperature for 2 h. The mixture was quenched with water and extracted with ethyl acetate. The organic layer was dried over sodium sulfate, filtered, and concentrated under reduced pressure. The resulting residue was purified by silica gel chromatography (CH_2Cl_2/MeOH 99:1 v:v) to give **7h** (530 mg, 72%) as an amber oil. ^{1}H NMR (300 MHz, $CDCl_3$) δ 7.71 (dd, J = 7.2, 1.9 Hz, 1H), 7.35 (m, 5H), 7.29 (dd, J = 7.2, 1.9 Hz, 1H), 6.05 (t, J = 7.0 Hz, 1H), 5.18 (s, 2H).

Synthesis of 3-bromo-1-(4-methoxybenzyl)pyridin-2(1*H*)-one (7i)

Compound **7i** was prepared from 4-methoxybenzyl bromide and compound **5** following the same procedure as described for the synthesis of compound **7h**. White solid (81%). ^{1}H NMR (400 MHz, $CDCl_3$) δ 7.69 (d, J = 7.2 Hz, 1H), 7.29 (dd, J = 5.5, 3.2 Hz, 3H), 6.87 (d, J = 8.5 Hz, 2H), 6.04 (t, J = 7.0 Hz, 1H), 5.11 (s, 2H), 3.79 (s, 3H).

Synthesis of 3-bromo-1-ethylpyridin-2(1*H*)-one (7j)

A mixture of 3-bromopyridin-2(1*H*)-one (**5**) (200 mg, 1.2 mmol), potassium carbonate (497 mg, 3.6 mmol), and iodoethane (561 mg, 3.6 mmol) in DMF (10 mL) was heated at 80 °C for 2 h. The reaction was concentrated

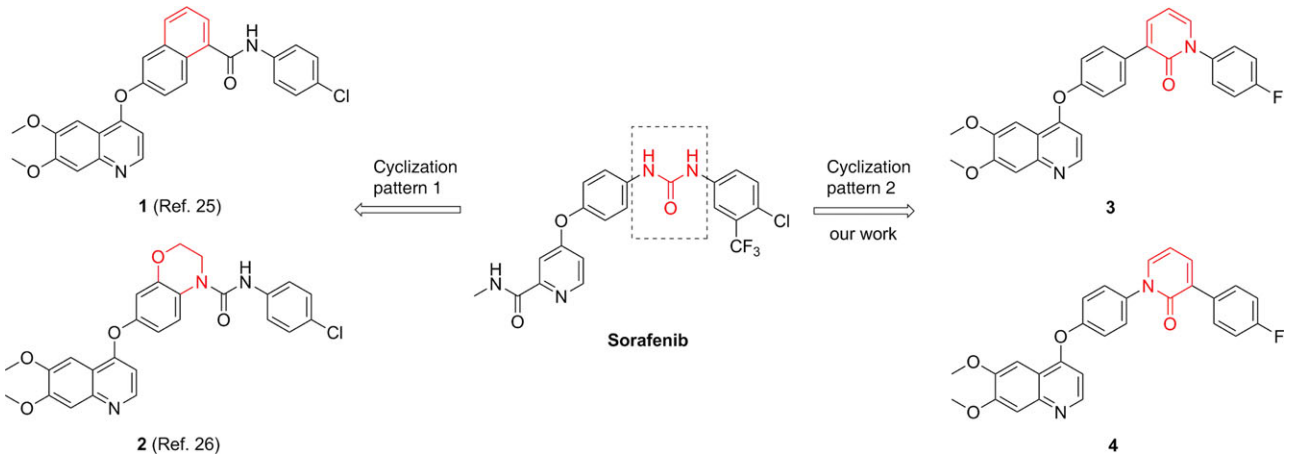

Figure 1: Different cyclization patterns of urea moiety.

under reduced pressure, and the resulting residue was purified by silica gel chromatography (CH_2Cl_2/MeOH 99:1 v:v) to give **7j** (115 mg, 52%) as an amber oil. ^{1}H NMR (400 MHz, $CDCl_3$) δ 7.72 (d, J = 7.2 Hz, 1H), 7.29 (d, J = 6.7 Hz, 1H), 6.08 (t, J = 7.0 Hz, 1H), 4.04 (q, J = 7.2 Hz, 2H), 1.37 (t, J = 7.2 Hz, 3H).

Synthesis of 3-bromo-1-methylpyridin-2(1*H*)-one (7k)

Compound **7k** was prepared from **5** and iodomethane following the same procedure as described for the synthesis of compound **7j**. Amber oil (60%). ^{1}H NMR (300 MHz, $CDCl_3$) δ 7.73 (d, J = 7.2 Hz, 1H), 7.29 (d, J = 6.7 Hz, 1H), 6.06 (t, J = 7.4 Hz, 1H), 3.61 (s, 3H).

General procedure for the synthesis of compounds 10, 33a and 33d–i

A mixture of 4-chloro-6,7-dimethoxyquinoline (**8**) (1 g, 4.5 mmol) and 4-bromophenol (2.3 g, 13.4 mmol) was heated at 170 °C for an hour. The resulting mixture was dissolved in ethyl acetate (50 mL) and washed with water and brine successively. The organic layer was dried over sodium sulfate, filtered, and concentrated under reduced pressure. The resulting residue was purified by silica gel chromatography (CH_2Cl_2/MeOH 98:2 v:v) to give **10** (1.44 g, 89%) as a yellow solid. ^{1}H NMR (300 MHz, $CDCl_3$) δ 8.49 (d, J = 5.2 Hz, 1H), 7.56 (d, J = 9.0 Hz, 2H), 7.49 (s, 1H), 7.41 (s, 1H), 7.06 (d, J = 8.9 Hz, 2H), 6.46 (d, J = 5.3 Hz, 1H), 4.04 (s, 3H), 4.02 (s, 3H).

Compounds **33a** and **33d–i** were prepared following the same procedure as described for the synthesis of compound **10**, and the analytical data were summarized in the supporting information.

Synthesis of 4-((4-bromophenyl)thio)-6,7-dimethoxyquinoline (33b)

To a mixture of **8** (200 mg, 0.9 mmol) and 4-bromobenzenethiol (338 mg, 1.8 mmol) in DMF (10 mL) was added triethylamine (270 mg, 2.8 mmol). The reaction mixture was stirred at ambient temperature for 3 h. The reaction mixture was concentrated under reduced pressure, and the resulting residue was purified by silica gel chromatography (CH_2Cl_2/MeOH 99:1–97:3 v:v) to give **33b** (200 mg, 60%) as a white solid. ^{1}H NMR (300 MHz, $CDCl_3$) δ 8.47 (d, J = 4.9 Hz, 1H), 7.55 (d, J = 8.5 Hz, 2H), 7.41 (s, 1H), 7.37 (m, 3H), 6.81 (d, J = 4.8 Hz, 1H), 4.04 (s, 3H), 4.01 (s, 3H).

Synthesis of *N*-(4-bromophenyl)-6,7-dimethoxyquinolin-4-amine (33c)

To a mixture of **8** (100 mg, 0.45 mmol) and 4-bromoaniline (93 mg, 0.54 mmol) in isopropyl alcohol (5 mL) was added one drop of concentrated HCl. The reaction mixture was heated at 120 °C in a sealed tube for 2 h. The reaction mixture was filtrated, and the filter cake was washed with ethyl acetate to give **33c** (130 mg, 81%) as a pale-yellow solid. ^{1}H NMR (400 MHz, DMSO) δ 10.71 (s, 1H), 8.37 (d, J = 6.9 Hz, 1H), 8.14 (s, 1H), 7.75 (d, J = 8.6 Hz, 2H), 7.46 (d, J = 9.0 Hz, 3H), 6.78 (d, J = 6.9 Hz, 1H), 4.00 (s, 3H), 3.98 (s, 3H).

General procedure for the synthesis of compounds 11 and 34

A mixture of **10** (500 mg, 1.4 mmol), bis(pinacolato)diboron (529 mg, 2.1 mmol), and potassium acetate (409 mg, 4.2 mmol) was bubbled with argon for 10 min. $Pd(dppf)_2Cl_2$ (50 mg, 0.07 mmol) was added, and the reaction mixture was heated at 90 °C for 2 h. The reaction mixture was concentrated under reduced pressure, and the resulting residue was purified by silica gel chromatography (CH_2Cl_2/MeOH 99:1–98:2 v:v) to give **11** (560 mg, 99%) as a yellow solid. ^{1}H NMR (300 MHz, $CDCl_3$) δ 8.48 (d, J = 5.3 Hz, 1H), 7.90 (d, J = 8.6 Hz, 2H), 7.52 (s, 1H), 7.42 (s, 1H), 7.17 (d, J = 8.6 Hz, 2H), 6.49 (d, J = 5.3 Hz, 1H), 4.04 (s, 3H), 4.02 (s, 3H), 1.36 (s, 12H).

Compounds of **34** were prepared following the same procedure as described for the synthesis of compound **11**, and the analytical data were summarized in supporting information.

General procedure for the synthesis of compounds 3, 12–21 and 35

A mixture of **11** (81 mg, 0.2 mmol), **7a** (50 mg, 0.2 mmol), and cesium carbonate (409 mg, 0.4 mmol) was bubbled with argon for 10 min. $Pd(PPh_3)_2Cl_2$ (9 mg, 0.01 mmol) was added, and the reaction mixture was heated at 60 °C for 2 h. The reaction mixture was concentrated under reduced pressure, and the resulting residue was purified by silica gel chromatography (CH_2Cl_2/MeOH 99:1–98:2 v:v) to give **3** (52 mg, 56%) as a white solid, mp: 200–202 °C. ^{1}H NMR (300 MHz, $CDCl_3$) δ 8.49 (d, J = 5.3 Hz, 1H), 7.84 (d, J = 8.7 Hz, 2H), 7.63 (dd, J = 7.0, 2.0 Hz, 1H), 7.55 (s, 1H), 7.46–7.36 (m, 4H), 7.24–7.16 (m, 4H), 6.56 (d, J = 5.3 Hz, 1H), 6.39 (t, J = 6.9 Hz, 1H), 4.05 (s, 6H). ^{13}C NMR (126 MHz, $CDCl_3$) δ 162.4 (d, J_{C-F} = 287.0 Hz), 161.6, 160.5, 154.5, 153.0, 149.7, 149.1, 147.1, 138.1, 137.3, 137.2 (d, J_{C-F} = 2.8 Hz), 133.8, 131.7, 130.7 (2C), 128.7 (d, J_{C-F} = 8.7 Hz, 2C), 120.7 (2C), 116.4, 116.4 (d, J_{C-F} = 23.2 Hz, 2C), 108.0, 106.4, 104.1, 99.6, 56.3 (2C). HRMS (EI$^+$) *m/z* calcd for $C_{28}H_{21}FN_2O_4$ 468.1485; found 468.1475.

Compounds **12–21** and **35** were prepared following the same procedure as described for the synthesis of compound **3**, and the analytical data were summarized in supporting information.

Synthesis of 3-(4-fluorophenyl)-1-(4-methoxyphenyl)pyridin-2(1*H*)-one (22)

Compound **22** was prepared from **6a** and **7d** following the same procedure as described for the synthesis of compound **3**. White solid (77%). ^{1}H NMR (300 MHz, CDCl3) δ 7.72 (dd, J = 8.7, 5.5 Hz, 2H), 7.53 (dd, J = 7.0, 2.0 Hz, 1H), 7.38–7.30 (m, 3H), 7.07 (t, J = 8.7 Hz, 2H), 6.99 (d, J = 8.9 Hz, 2H), 6.32 (t, J = 6.9 Hz, 1H), 3.85 (s, 3H).

Synthesis of 3-(4-fluorophenyl)-1-(4-hydroxyphenyl)pyridin-2(1*H*)-one (23)

Boron tribromide (424 mg, 1.7 mmol) was added dropwise to a solution of **22** (100 mg, 0.3 mmol) in CH_2Cl_2 (5 mL) at 0 °C. The resulting reaction mixture was stirred at ambient temperature overnight. CH_2Cl_2 (20 mL) was added to the mixture, and the resulting solution was washed with saturated aq $NaHCO_3$, water and brine successively. The organic layer was dried over sodium sulfate, filtered, and concentrated under reduced pressure. The resulting residue was purified by silica gel chromatography (CH_2Cl_2/MeOH 99:1–97:3 v:v) to give **23** (75 mg, 79%) as a white solid. ^{1}H NMR (300 MHz, DMSO) δ 9.76 (s, 1H), 7.74 (dd, J = 8.4, 5.8 Hz, 2H), 7.71–7.58 (m, 2H), 7.27–7.15 (m, 4H), 6.86 (d, J = 8.6 Hz, 2H), 6.38 (t, J = 6.9 Hz, 1H).

Synthesis of 1-(4-((6,7-dimethoxyquinolin-4-yl)oxy) phenyl)-3-(4-fluorophenyl)pyridin-2(1*H*)-one (4)

A mixture of **8** (22 mg, 0.1 mmol), **23** (28 mg, 0.1 mmol), and 4-dimethylaminopyridine (12 mg, 0.1 mmol) in toluene (2 mL) and chloroform (1 mL) was heated to 180 °C for an hour under microwave irradiation. The reaction mixture was concentrated, and the residue was purified by silica gel chromatography (CH_2Cl_2/MeOH 99:1–97:3 v:v) to give **4** (30 mg, 64%) as a white solid, mp: 228–230 °C. ^{1}H NMR (300 MHz, $CDCl_3$) δ 8.53 (d, J = 5.2 Hz, 1H), 7.76–7.69 (m, 2H), 7.60–7.49 (m, 4H), 7.46–7.41 (m, 2H), 7.31 (d, J = 8.8 Hz, 2H), 7.09 (t, J = 8.8 Hz, 2H), 6.62 (d, J = 5.2 Hz, 1H), 6.40 (t, J = 6.9 Hz, 1H), 4.05 (s, 6H). ^{13}C NMR (126 MHz, $CDCl_3$) δ 162.6 (d, J_{C-F} = 248.2 Hz), 161.5, 160.1, 154.6, 153.1, 149.8, 148.7, 146.9, 138.1, 137.9, 136.9, 132.4 (d, J_{C-F} = 3.2 Hz), 131.7, 130.5 (d, J_{C-F} = 8.1 Hz, 2C), 128.7 (2C), 121.5 (2C), 116.3, 115.0 (d, J_{C-F} = 21.3 Hz, 2C), 107.7, 106.5, 104.3, 99.3, 56.2 (2C). HRMS (EI$^+$) m/z calcd for $C_{28}H_{21}FN_2O_4$ 468.1485; found 468.1481.

Compounds **8** and **24** were synthesized according to literature procedures (29).

Biological evaluation

Enzyme-linked immunosorbent assay (ELISA)

The kinase domain of VEGFR-2 was expressed using the Bac-to-Bac™ baculovirus expression system and purified on Ni-NTA columns. The ability of the compounds to inhibit the activity of VEGFR-2 was tested by ELISA. The substrate of poly (Glu, Tyr) 4:1 (20 μg/mL) (Sigma, St. Louis, MO, USA) was precoated in 96-well ELISA plates, and the kinase was incubated with the compounds in reaction buffer (50 mM HEPES pH 7.4, 20 mM $MgCl_2$, 0.1 mM $MnCl_2$, 0.2 mM Na_3VO_4, 1 mM DTT) containing 10 μM ATP at 37 °C for an hour. The plates were washed with PBS and incubated with antiphosphotyrosine (PY99) antibody (Santa Cruz Biotechnology, Santa Cruz, CA, USA) and horseradish peroxidase-conjugated antibody (Calbiochem, SanDiego, CA, USA) successively. The results were visualized using *o*-phenylenediamine (OPD) and read on a multiwell spectrophotometer (VERSAmax™; Molecular Devices, Sunnyvale, CA, USA).

Western blotting

The HUVECs were obtained from ScienCell Research Laboratories (Santiago, CA, USA). To determine the inhibitory activities of the compounds on the VEGF-induced VEGFR phosphorylation, HUVECs were seeded in the 6-well plates and were cultured overnight. Then, the cells were starved for 24 h with endothelial cell basal medium which contained no serum. The HUVECs were treated with the compounds for 2 h and then stimulated with 100 ng/mL recombinant human $VEGF_{165}$ (R&D Systems, Abingdon, UK) for 15 min. Subsequently, the HUVECs were lysed with 1 × SDS lysis buffer and were processed for Western blot analysis. The intensities of each band on Western blot results were quantified by IMAGE J software (National Institutes of Health, Bethesda, MD, USA).

Tube formation assay

The standard BD Matrigel matrix (BD Biosciences, Billerica, MA, USA) was coated into 96-well plates and incubated at 37 °C. HUVECs were seeded into Matrigel-coated plates together with $VEGF_{165}$ (100 ng/mL) and different concentration of compounds. After the HUVECs were incubated at 37 °C for 8 h, photographs of the tube network formation were taken on a OLYMPUS IX51 stereoscope (Tokyo, Japan). The numbers of the intact tubes were counted manually of each full field.

Molecular modeling

Prior to the docking study, protein structure of VEGFR-2 (PDB ID: 3B8Q) was prepared using the Protein Preparation Wizard Workflow provided in MAESTRO 9.0 and the default settings were used[a]. A grid box was built with the size of 20 Å^3, centered on the cocrystal ligand located in the ATP-binding site of VEGFR-2. Both compound **17** and the ligand from the cocrystal structure were prepared with LIGPREP[b] to generate low-energy 3D conformations and to determine probable ionization states at pH 7.0 ± 2.0. A redocking run was performed to evaluate the performance of the docking protocol employing GLIDE 5.5[c] with extra precision (XP) (30) mode. Upon validation (RMSD = 0.134),

compound **17** was docked into the ATP-binding site of VEGFR-2 using the same method. Figure 4 was generated by PYMOL (Version 1.3r1)[d].

Results and Discussion

Chemistry

As depicted in Schemes 1 and 2, intermediates **7a**–**k** were prepared from **5** via Chan-Lam coupling reaction (**7a**–**g**) or nucleophilic substitution reactions (**7h**–**k**) in good to excellent yields. Conversion from 4-chloro-6,7-dimethoxyquinoline (**8**) to bromide **10** with 4-bromophenol and a following boration reaction with bis(pinacolato)diboron gave boronic ester **11**, which was then coupled with **7a**–**k** to generate compounds **3** and **12**–**21**. Coupling of **6a** with **7d** gave ether **22**, which was subsequently treated with boron tribromide to furnish phenol **23**. Compound **4** was obtained by heating the mixture of **8** and **23** under microwave irradiation at 180 °C in toluene and chloroform using 4-dimethylaminopyridine as the catalyst. Derivatives **35** were smoothly obtained following the same route as described for compound **3** by starting from the appropriate chlorides (**8** or **24**) and nucleophiles (**9** or **25**–**32**) as illustrated in Scheme 3. As observed in the Suzuki coupling reaction step, the yields (60–72%) of the 3′-substituted derivatives (**35d**, **35f**, and **35h**) were comparable to the unsubstituted derivative **17**, while the 2′-substituted derivatives (**35e**, **35g**, and **35i**) gave much lower yields (11–25%) due to the steric hindrance effect.

Kinase inhibitory activity

Isomers **3** and **4** were prepared as proof of concept compounds. As detailed in Table 1, compound **3** demonstrated potent VEGFR-2 inhibitory activity possessing an IC_{50} value of 6.9 nM. However, the inhibitory activity of compound **4** was much weaker (IC_{50} > 100 nM). This result indicated that the substitution pattern of the pyridone moiety was an important factor that influenced VEGFR-2 inhibitory activity. Compound **12**, with no substituents on the terminal phenyl ring, displayed a slight decrease in potency compared with compound **3**, implying that inclusion of substituents on the terminal phenyl ring had favorable impacts on the activity.

Compound **12** served as a benchmark during the initial optimization stage. Several compounds with different substitution patterns were designed and synthesized (Table 1). The 3-fluorine analogue **13** was equipotent to compound **3**. Slight increases in potency were observed in the methoxyl analogues **14** and **15**. Displacement of fluorine with chlorine led to a twofold enhancement in potency (**16** and **17**). Benzyl derivative **18** was fivefold less active than **12**, while the IC_{50} value of 4-methoxyl benzyl derivative **19** was > 100 nM. These results indicated that the distance between pyridone and the terminal phenyl ring was strictly restricted. Displacement of the terminal phenyl (**12**) with ethyl (**20**) or methyl (**21**) resulted in significant losses of activity (IC_{50} > 100 nM), which indicated the small lipophilic substituents were insufficient to occupy the hydrophobic pocket. To further explore the structure activity relationships (SARs), we selected 3-position chlorine as the default substituent of the terminal phenyl ring.

Quinazoline was also utilized as an important scaffold in VEGFR-2 inhibitors (31,32). However, as detailed in Table 2, the quinazoline derivative **35a** displayed a twofold decline in potency compared with quinoline **17**. Optimization of the linker atom between the 6,7-dimethoxyquinoline core and the middle phenyl ring demonstrated that an oxygen linker is preferred to the sulfur or nitrogen one. Compared with the oxygen linker derivative **17**, the sulfur or amino linker derivatives (**35b**–**c**) exhibited twofold to sixfold drops in potency.

The effects of substituents on the middle phenyl group were also investigated. The electronic properties of the substituents had minimal influence on potency; chlorine (**35d** and **35e**) or methoxyl (**35f** and **35g**) derivatives displayed similar inhibitory effects against VEGFR-2 (Table 2). But they were sixfold to ninefold less active compared with the

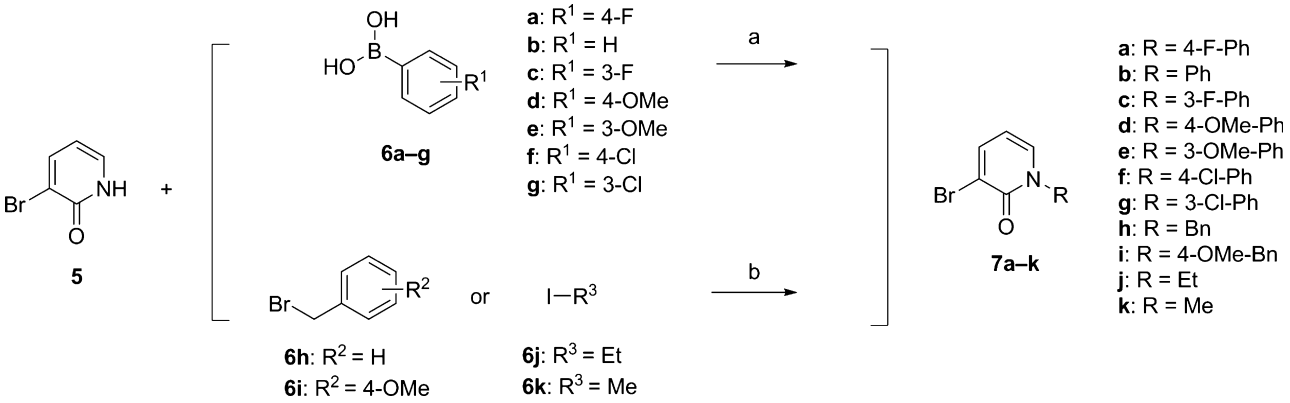

Scheme 1: Synthesis of compounds **7a**–**k**. Reagents and conditions: (a) $Cu(OAc)_2$, Py, 4 Å molecular sieve, O_2, CH_2Cl_2, r.t., 75%–88%; (b) for **7h**–**i**, NaH, DMF, 0 °C to r.t., 72–81%; for **7j**–**k**, K_2CO_3, DMF, 80 °C, 52–60%.

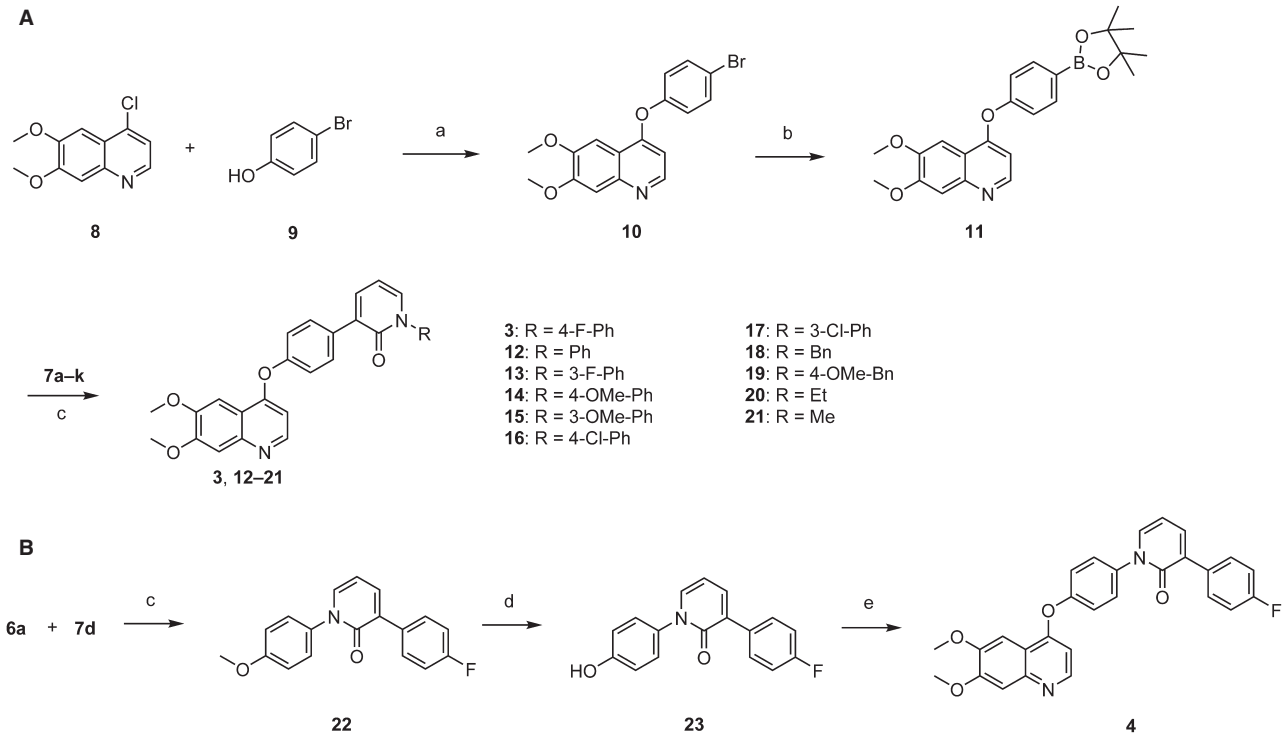

Scheme 2: Synthesis of compounds **3**, **4**, and **12**–**21**. Reagents and conditions: (a) neat, 160 °C, 89%; (b) B_2pin_2, $Pd(dppf)_2Cl_2$, KOAc, dioxane, 90 °C, 95%; (c) Cs_2CO_3, $Pd(PPh_3)_2Cl_2$, DMF, 60 °C, 45–80%; (d) BBr_3, CH_2Cl_2, 0 °C to r.t., 79%; (e) **8**, 4-DMAP, toluene, $CHCl_3$, 180 °C, microwave irradiation, 64%.

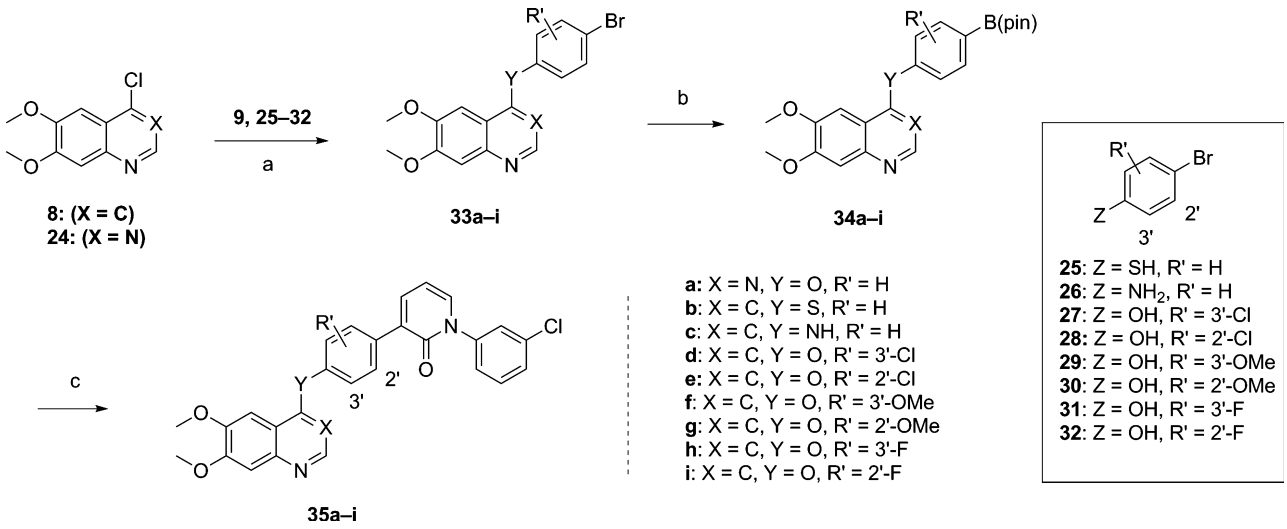

Scheme 3: Synthesis of compounds **35a**–**i**. Reagents and conditions: (a) for **33a** and **33d**–**i**, neat, 170 °C, 80–89%; for **33b**, Et_3N, DMF, r.t., 60%; for **33c**, conc. HCl, *i*-PrOH, 120 °C sealed tube, 81%; (b) B_2pin_2, $Pd(dppf)_2Cl_2$, KOAc, dioxane, 90 °C, 80–99%; (c) **7g**, Cs_2CO_3, $Pd(PPh_3)_2Cl_2$, DMF, 60 °C, 11–72%.

unsubstituted compound **17**, which may suggest bulky substituents were not well tolerated at this site: The chlorine or methoxyl may be relatively too big to occupy the binding pocket around the middle phenyl ring; the steric hindrance effect between the chlorine or methoxyl and the pyridone moiety may destabilize the active conformations. On the contrary, the smaller fluorine derivatives (**35h** and **35i**) slightly increased or retained VEGFR-2 potency. In consideration of their excellent VEGFR-2 inhibitory activities, we selected compounds **17** and **35h** for further evaluation.

Table 1: VEGFR-2 kinase inhibitory activity of compounds **3**, **4**, and **12**–**21**

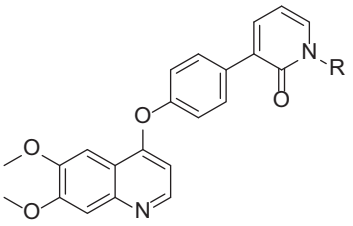

Compound	R	VEGFR-2 IC_{50} (nM)[a]
3	4-F-Ph	6.9 ± 1.6
4	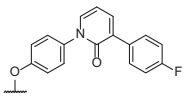	> 100
12	Ph	8.0 ± 1.5
13	3-F-Ph	6.1 ± 0.7
14	4-OMe-Ph	5.3 ± 1.1
15	3-OMe-Ph	4.8 ± 0.0
16	4-Cl-Ph	4.0 ± 0.7
17	3-Cl-Ph	3.5 ± 0.1
18	Bn	41.9 ± 0.4
19	4-OMe-Bn	> 100
20	Et	> 100
21	Me	> 100
Su11248	–	13.0 ± 1.1

[a]IC_{50} values were represented as the mean ± SD of two or more independent experiments.

Table 2: VEGFR-2 kinase inhibitory activity of compounds **17** and **35**

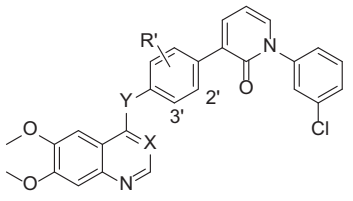

Compound	X	Y	R'	VEGFR-2 IC_{50} (nM)[a]
17	C	O	H	3.5 ± 0.1
35a	N	O	H	7.8 ± 0.9
35b	C	S	H	7.6 ± 1.2
35c	C	NH	H	23.6 ± 2.2
35d	C	O	3′-Cl	25.0 ± 3.2
35e	C	O	2′-Cl	36.6 ± 3.8
35f	C	O	3′-OMe	22.8 ± 3.1
35g	C	O	2′-OMe	26.5 ± 4.5
35h	C	O	3′-F	3.0 ± 1.2
35i	C	O	2′-F	3.6 ± 0.6
Su11248	–	–	–	13.0 ± 1.1

[a]IC_{50} values were represented as the mean ± SD of two or more independent experiments.

Western blotting and tube formation study

We subsequently examined the ability of compounds **17** and **35h** to inhibit the activation of VEGFR-2 and downstream Erk in HUVECs. As illustrated in Figure 2, compounds **17** and **35h** dose dependently suppressed the VEGF-induced phosphorylations of VEGFR-2 and Erk in HUVECs. The approved multikinase inhibitor sorafenib was used as a positive control. It was found that both compounds **17** and **35h** were more potent than sorafenib at the concentration of 100 nM and compound **35h** significantly inhibited VEGFR-2 phosphorylation at the concentration of 10 nM. These results indicated that compounds **17** and **35h** could block the VEGFR and Erk signaling pathways.

Tube formation by endothelial cells plays an important role in angiogenesis. Therefore, we investigated the *in vitro* anti-angiogenic effect of compounds **17** and **35h** in a tube formation assay. HUVECs were planted on Matrigel and treated with compounds **17** or **35h** at different concentrations in the presence of VEGF. As shown in Figure 3, both compounds dose dependently inhibited the VEGF-induced HUVEC tube formation and were more potent than sorafenib. Meanwhile, the cytotoxicity of both compounds was also tested, and they showed no obvious cytotoxicity on HUVECs under the same experimental condition (data not shown), which ruled out the possibility that cytotoxicity was involved in the inhibition of tube formation. These findings revealed that compounds **17** and **35h** were potent VEGFR-2 inhibitors at the cellular level.

Molecular docking study

To gain insight into the ligand–protein interactions, we performed a molecular docking study of compound **17** using a reported crystal structure of VEGFR-2 kinase domain (PDB ID: 3B8Q) (25). As depicted in Figure 4, compound **17** bound to the ATP-binding site of VEGFR-2. The 6,7-dimethoxyquinoline core engaged the linker region of the enzyme in a hydrogen bond between the nitrogen and Cys-919 (3.0 Å). The carbonyl group of the pyridone participated in a hydrogen bond contact with the backbone NH of Asp-1046 (2.7 Å), enabling the terminal 3-chlorophenyl ring to reside in the extended hydrophobic pocket. Additional van der Waals interaction was seen with the central phenyl ring and the surrounding lipophilic residues. This binding model disclosed the interaction patterns of the 1,3-diaryl-pyridone derivatives with VEGFR-2 and was consistent with our experimental data.

Conclusion

In conclusion, we have developed a series of 1,3-diaryl-pyridone derivatives as novel VEGFR-2 inhibitors. Compounds **17** and **35h** exhibited excellent VEGFR-2 inhibitory activity in enzymatic assays with IC_{50} values of 3.5 and 3.0 nM, respectively. In addition, these two compounds inhibited VEGF-induced HUVEC tube formation and suppressed activation of VEGFR-2 and downstream Erk signaling. Docking simulation showed that compound **17** was

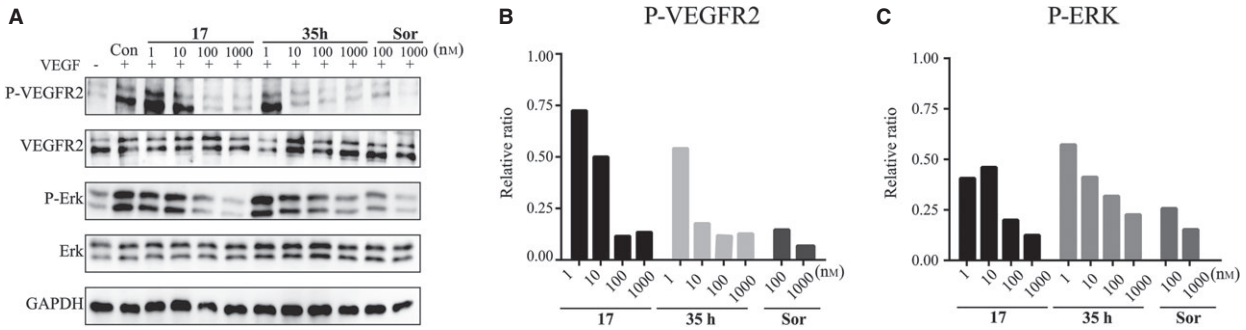

Figure 2: (A) Compounds **17** and **35h** inhibited the VEGF-induced activation of VEGFR-2 and Erk signaling in HUVECs. (B) The density of p-VEGFR bands was measured, and the ratios to VEGFR were calculated. (C) The density of p-ERK bands was measured, and the ratios to ERK were calculated. Sor: Sorafenib.

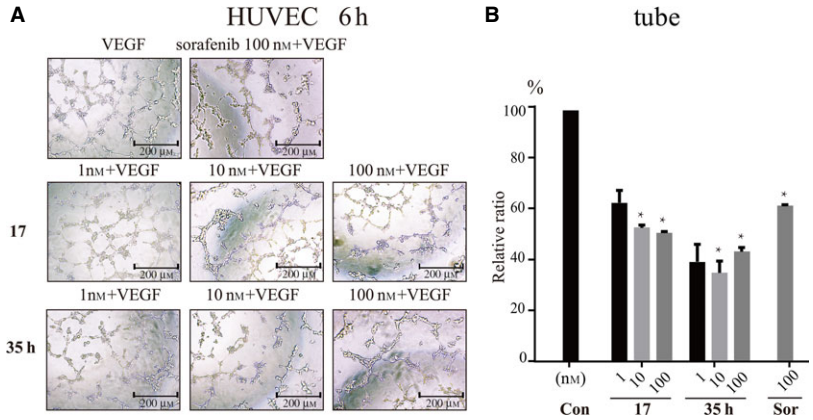

Figure 3: (A) Compounds **17** and **35h** inhibited the tube formation in HUVECs. (B) Numbers of the blood vessels in HUVEC assay were counted. Sor: Sorafenib. The asterisk (*) indicates a significant decrease of tube formation of cells treated with compounds compared with the DMSO-treated control group.

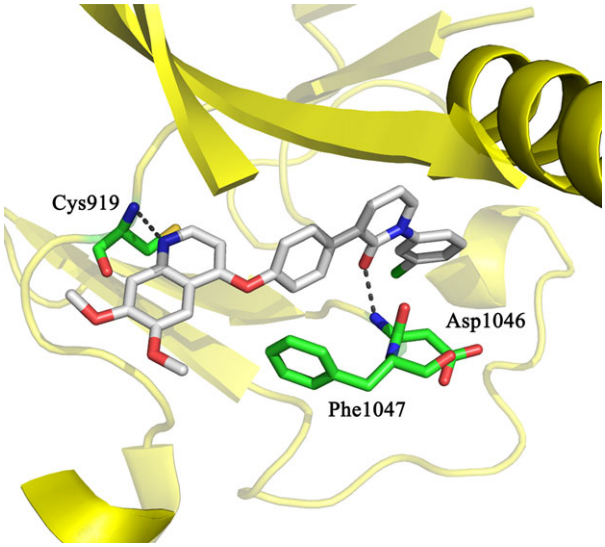

Figure 4: Predicted binding mode for compound **17** within the ATP-binding site of VEGFR-2.

anchored into the active site of VEGFR-2 via two critical hydrogen bonds and hydrophobic interactions. The results of this study indicated that 1,3-diaryl-pyridone was a promising scaffold for the development of novel VEGFR-2 inhibitors.

Acknowledgments

We thank the National Natural Science Foundation of China (Nos. 81273365, 81173080 and 81321092), National Science & Technology Major Project 'Key New Drug Creation and Manufacturing Program' (Nos. 2012ZX09103101-024 and 2014ZX09304002-008-001), Chinese National Programs for High Technology Research and Development (No. 2012AA020302), and the Shanghai Science and Technology Commission (No. 1315431901300) for their financial support.

Conflict of Interests

The authors declared no conflict of interests.

References

1. Folkman J. (1971) Tumor angiogenesis: therapeutic implications. N Engl J Med;285:1182–1186.

2. Hanahan D., Folkman J. (1996) Patterns and emerging mechanisms of the angiogenic switch during tumorigenesis. Cell;86:353–364.
3. Hanahan D., Weinberg R.A. (2000) The hallmarks of cancer. Cell;100:57–70.
4. Kerbel R.S. (2000) Tumor angiogenesis: past, present and the near future. Carcinogenesis;21:505–515.
5. Musumeci F., Radi M., Brullo C., Schenone S. (2012) Vascular endothelial growth factor (VEGF) receptors: drugs and new inhibitors. J Med Chem;55:10797–10822.
6. Ferrara N., Kerbel R.S. (2005) Angiogenesis as a therapeutic target. Nature;438:967–974.
7. Kerbel R.S. (2006) Antiangiogenic therapy: a universal chemosensitization strategy for cancer? Science;312:1171–1175.
8. Des Guetz G., Uzzan B., Nicolas P., Cucherat M., Morere J.F., Benamouzig R., Breau J.L., Perret G.Y. (2006) Microvessel density and VEGF expression are prognostic factors in colorectal cancer. Meta-analysis of the literature. Br J Cancer;94:1823–1832.
9. Rahimi N. (2006) Vascular endothelial growth factor receptors: molecular mechanisms of activation and therapeutic potentials. Exp Eye Res;83:1005–1016.
10. Roskoski R. Jr (2008) VEGF receptor protein-tyrosine kinases: structure and regulation. Biochem Biophys Res Commun;375:287–291.
11. Olsson A.K., Dimberg A., Kreuger J., Claesson-Welsh L. (2006) VEGF receptor signalling—in control of vascular function. Nat Rev Mol Cell Biol;7:359–371.
12. Roy H., Bhardwaj S., Yla-Herttuala S. (2006) Biology of vascular endothelial growth factors. FEBS Lett;580:2879–2887.
13. Izzedine H., Buhaescu I., Rixe O., Deray G. (2007) Sunitinib malate. Cancer Chemother Pharmacol;60:357–364.
14. Ahmad T., Eisen T. (2004) Kinase inhibition with BAY 43-9006 in renal cell carcinoma. Clin Cancer Res;10:6388S–6392S.
15. Harris P.A., Boloor A., Cheung M., Kumar R., Crosby R.M., Davis-Ward R.G., Epperly A.H. *et al.* (2008) Discovery of 5-[[4-[(2,3-dimethyl-2*H*-indazol-6-yl)methylamino]-2-pyrimidinyl]amino]-2-methyl-benzenesulfonamide (Pazopanib), a novel and potent vascular endothelial growth factor receptor inhibitor. J Med Chem;51:4632–4640.
16. Eskens F.A., de Jonge M.J., Bhargava P., Isoe T., Cotreau M.M., Esteves B., Hayashi K., Burger H., Thomeer M., van Doorn L., Verweij J. (2011) Biologic and clinical activity of tivozanib (AV-951, KRN-951), a selective inhibitor of VEGF receptor-1, -2, and -3 tyrosine kinases, in a 4-week-on, 2-week-off schedule in patients with advanced solid tumors. Clin Cancer Res;17:7156–7163.
17. Dai Y., Hartandi K., Ji Z., Ahmed A.A., Albert D.H., Bauch J.L., Bouska J.J. *et al.* (2007) Discovery of *N*-(4-(3-amino-1*H*-indazol-4-yl)phenyl)-*N'*-(2-fluoro-5-methylphenyl)urea (ABT-869), a 3-aminoindazole-based orally active multitargeted receptor tyrosine kinase inhibitor. J Med Chem;50:1584–1597.
18. Shahin M.I., Abou El Ella D.A., Ismail N.S., Abouzid K.A. (2014) Design, synthesis and biological evaluation of type-II VEGFR-2 inhibitors based on quinoxaline scaffold. Bioorg Chem;56:16–26.
19. Yang L.L., Li G.B., Ma S., Zou C., Zhou S., Sun Q.Z., Cheng C., Chen X., Wang L.J., Feng S., Li L.L., Yang S.Y. (2013) Structure-activity relationship studies of pyrazolo[3,4-*d*]pyrimidine derivatives leading to the discovery of a novel multikinase inhibitor that potently inhibits FLT3 and VEGFR2 and evaluation of its activity against acute myeloid leukemia *in vitro* and *in vivo*. J Med Chem;56:1641–1655.
20. Sartini S., Coviello V., Bruno A., La Pietra V., Marinelli L., Simorini F., Taliani S. *et al.* (2014) Structure-based optimization of tyrosine kinase inhibitor CLM3. Design, synthesis, functional evaluation, and molecular modeling studies. J Med Chem;57:1225–1235.
21. Lin W.H., Hsu J.T., Hsieh S.Y., Chen C.T., Song J.S., Yen S.C., Hsu T. *et al.* (2013) Discovery of 3-phenyl-1*H*-5-pyrazolylamine derivatives containing a urea pharmacophore as potent and efficacious inhibitors of FMS-like tyrosine kinase-3 (FLT3). Bioorg Med Chem;21:2856–2867.
22. Choi H.E., Choi J.H., Lee J.Y., Kim J.H., Kim J.H., Lee J.K., Kim G.I., Park Y., Chi Y.H., Paik S.H., Lee J.H., Lee K.T. (2013) Synthesis and evaluation of nicotinamide derivative as anti-angiogenic agents. Bioorg Med Chem Lett;23:2083–2088.
23. Hirose M., Okaniwa M., Miyazaki T., Imada T., Ohashi T., Tanaka Y., Arita T. *et al.* (2012) Design and synthesis of novel DFG-out RAF/vascular endothelial growth factor receptor 2 (VEGFR2) inhibitors: 3. Evaluation of 5-amino-linked thiazolo[5,4-*d*]pyrimidine and thiazolo[5,4-*b*]pyridine derivatives. Bioorg Med Chem;20:5600–5615.
24. McTigue M., Murray B.W., Chen J.H., Deng Y.L., Solowiej J., Kania R.S. (2012) Molecular conformations, interactions, and properties associated with drug efficiency and clinical performance among VEGFR TK inhibitors. Proc Natl Acad Sci USA;109:18281–18289.
25. Harmange J.C., Weiss M.M., Germain J., Polverino A.J., Borg G., Bready J., Chen D. *et al.* (2008) Naphthamides as novel and potent vascular endothelial growth factor receptor tyrosine kinase inhibitors: design, synthesis, and evaluation. J Med Chem;51:1649–1667.
26. La D.S., Belzile J., Bready J.V., Coxon A., DeMelfi T., Doerr N., Estrada J. *et al.* (2008) Novel 2,3-dihydro-1,4-benzoxazines as potent and orally bioavailable inhibitors of tumor-driven angiogenesis. J Med Chem;51:1695–1705.
27. Lv Y., Li M., Liu T., Tong L., Peng T., Wei L., Ding J., Xie H., Duan W. (2014) Discovery of a new series of naphthamides as potent VEGFR-2 kinase inhibitors. ACS Med Chem Lett;5:592–597.

28. Kossen K., Seiwert S.D., Serebryany V., Ruhrmund D., Beigelman L., Raveglia L.F.M., Vallese S., Bianchi I., Hu T. (2009) Compounds and methods for treating inflammatory and fibrotic disorders, USA Patent No. WO 2009149188.
29. Furuta T., Sakai T., Senga T., Osawa T., Kubo K., Shimizu T., Suzuki R., Yoshino T., Endo M., Miwa A. (2006) Identification of potent and selective inhibitors of PDGF receptor autophosphorylation. J Med Chem;49:2186–2192.
30. Friesner R.A., Murphy R.B., Repasky M.P., Frye L.L., Greenwood J.R., Halgren T.A., Sanschagrin P.C., Mainz D.T. (2006) Extra precision glide: docking and scoring incorporating a model of hydrophobic enclosure for protein–ligand complexes. J Med Chem;49:6177–6196.
31. Sorbera L.A., Serradell N., Rosa E., Bolos J., Bayes M. (2007) Cediranib—VEGFR inhibitor, antiangiogenic agent, oncolytic. Drug Fut;32:577–589.
32. Ple P.A., Jung F., Ashton S., Hennequin L., Laine R., Morgentin R., Pasquet G., Taylor S. (2012) Discovery of AZD2932, a new quinazoline ether inhibitor with high affinity for VEGFR-2 and PDGFR tyrosine kinases. Bioorg Med Chem Lett;22:262–266.

Notes

[a]Maestro, version 9.0 (2009) Schrödinger, LLC, New York, NY, USA.
[b]LigPrep, version 2.3 (2009) Schrödinger, LLC, New York, NY, USA.
[c]Glide, version 5.5 (2009) Schrödinger, LLC, New York, NY, USA.
[d]The PyMOL Molecular Graphics System, Version 1.3r1 (2010) Schrodinger, LLC, New York, NY, USA.

Supporting Information

Additional Supporting Information may be found in the online version of this article:

Data S1. Analytical data for compounds **7**, **12**–**21**, and **33**–**35**.